Available online at www.sciencedirect.com

ScienceDirect

IFAC Papers Online CONFERENCE PAPER ARCHIVE

IFAC PapersOnLine 58-4 (2024) 556–561

Learning-based MPC with uncertainty estimation for resilient microgrid energy management ⋆

Vittorio Casagrande * **Martin Ferianc** * **Miguel Rodrigues** * **Francesca Boem** *

* *Dept. of Electronic and Electrical Engineering, University College London, London, United Kingdom (e-mail: {vittorio.casagrande.19, martin.ferianc.19,m.rodrigues,f.boem}@ucl.ac.uk)*

Abstract: To enhance fault resilience in microgrid systems at the energy management level, this paper introduces a novel proactive scheduling algorithm, based on uncertainty modelling thanks to a specifically designed neural network. The algorithm is trained and deployed online and it estimates uncertainties in predicting future load demands and other relevant profiles. We integrate the novel learning algorithm with a stochastic model predictive control, enabling the microgrid to store sufficient energy to adaptively deal with possible faults. Experimental results show that a reliable estimation of the unknown profiles' mean and variance is obtained, improving the robustness of proactive scheduling strategies against uncertainties.

Keywords: Energy Management Systems, Microgrid, Model Predictive Control, Online Learning, Uncertainty Estimation

1. INTRODUCTION

The microgrid concept was introduced in (Lasseter, 2002) to coordinate the operation of numerous distributed energy resources. Ensuring the microgrid's power resilience against possible faults is a critical priority (Panteli and Mancarella, 2015). Although a microgrid system inherently enhances overall system resilience due to its local generation and storage, designing a suitable controller that explicitly considers possible faults is crucial. At the tertiary control level, the Energy Management System (EMS) calculates the future power schedule for all agents connected to the microgrid. The main challenge in designing the EMS stems from the uncertainty associated with future renewable power generation, load demand, and electricity prices, which are typically unknown in advance. The possible presence of faults adds additional complexity to the controller design.

Fault resilience is addressed at the EMS level by implementing two main strategies: *proactive scheduling* and *outage management* (Hussain et al., 2019). Proactive scheduling ensures that the system can handle a fault effectively before its occurrence, while outage management instead focuses on managing the fault once it has occurred. Typically, the first strategy is implemented by storing enough energy in the microgrid to supply the loads during faults. In contrast, the second strategy optimally manages the stored energy under fault conditions. Besides reliable predictions of the future uncertain profiles, e.g. the future load demand, the robustness of a proactive scheduling strategy can be enhanced if knowledge about the uncertainty of such predictions is available.

In this paper, we design a resilient EMS to coordinate the operation of microgrid agents, explicitly considering the potential occurrence of a fault. In particular, we focus on implementing a proactive scheduling strategy against blackouts under uncertainty of future load demand and renewable generation. To address this challenge, we extend the online learning-based Model Predictive Control (MPC) algorithm, first presented in (Casagrande et al., 2023), to estimate the forecasts' mean and variance and consider this information in the scheduling computation. The proposed EMS is composed of two blocks: (i) a predictor that forecasts the future uncertain profiles as well as their uncertainty; (ii) an optimiser that implements a stochastic MPC algorithm with chance constraints. The learning algorithm outputs the mean and the variance of the unknown profiles while maintaining its ability to adapt online to possible changes, such as installing new load equipment or PV modules. The optimiser schedules the microgrid operation, employing the predicted profiles, to minimise the cost due to energy trading. The proactive scheduling strategy is implemented by enforcing the state of charge to be greater than the future load demand with a certain probability. By implementing this as a chance constraint, the uncertainty in the profile prediction and fault occurrence reduces the conservativeness of the proactive scheduling strategy.

In the literature, works concerning microgrid resilience at the EMS level propose proactive scheduling and out-

⋆ This work has been supported by the UK Engineering and Physical Sciences Research Council (grant reference: EP/W024411/1). For the purpose of open access, the author has applied a Creative Commons Attribution (CC BY) licence to any Author Accepted Manuscript version arising. Martin Ferianc was sponsored through a scholarship from the Institute of Communications and Connected Systems at UCL.

10.1016/j.ifacol.2024.07.277

age management strategies (Hussain et al., 2019). Outage management is typically obtained by reformulating the scheduling optimisation problem to include safety objectives (Haessig et al., 2019; Casagrande et al., 2022), by resorting to interconnections between microgrids (Pashajavid et al., 2015) or to different backup options for power generation (Bernardi et al., 2021). An outage management strategy is feasible only if enough energy is stored in the microgrid once the fault occurs, and this is indeed the goal of proactive scheduling. This strategy is implemented by storing an additional amount of energy to be used in the case of a fault. For example, in (Jongerden et al., 2016), a fixed percentage of the total storage capacity, (20-30%) is reserved for fault resilience. However, less storage capacity is available for other EMS objectives, such as economic goals, and the electricity bill increases. While acknowledging an increase in costs is necessary to implement a resilience strategy, these methods overlook the future energy requirement at the risk of storing too much or too little energy for the loads' requirements. Adapting the amount of backup energy to the future load demand is beneficial since only the required storage capacity is devoted to resiliency. In (Prodan et al., 2015), uncertainty is accounted for by weighting less the cost function terms that are farther in the future and hence more uncertain. In (Khodaei, 2014), a method to switch from grid-connected to island mode considering uncertainties in load demand and renewable generation is proposed against power outages, and uncertainty is addressed in a robust min-max optimisation method. These two works overlook the problem of predicting uncertain profiles by assuming to know them and their uncertainty band. Beyond the uncertainty in the predictions, the uncertainty in the fault occurrence should be considered too, to avoid storing a considerable amount of backup energy when the chance of fault occurrence is remote. The scenario-based approach has been proposed in (Tobajas et al., 2022; Casagrande and Boem, 2022) to take into account the probability of fault occurrence explicitly. The main drawback of this approach is that the generated scenario tree may lead to a large-scale optimisation problem (Casagrande and Boem, 2022). Instead, we consider a chance-constrained optimisation problem where the number of decision variables linearly depends on the prediction horizon only. Moreover, we consider the uncertain profiles' prediction. Compared to (Casagrande et al., 2022), the method proposed here is centralised instead of distributed and the problem of predicting uncertain profiles is considered. As opposed to (Prodan et al., 2015), we explicitly consider online-predicted uncertainty thresholds. By setting the probability of enforcing the proactive scheduling constraint greater than the probability of fault occurrence, we achieve a twofold objective, in contrast to (Tobajas et al., 2022): on the one hand, the constraint is violated with a higher probability when the chance of fault occurrence is low, i.e. when the backup energy is not required; on the other hand, the resilient EMS is robust against uncertainty in the predictions. Our algorithm is compatible with any method for fault probability estimation, such as fragility curves (Panteli et al., 2016).

The online learning method proposed in (Casagrande et al., 2023) is extended to estimate uncertainty. While there are several examples in the literature of methods to estimate future profiles relevant for microgrid EMS and offline-batch learning, few works propose methods for online uncertainty estimation. Methods for online uncertainty estimation are proposed in (Álvarez et al., 2021) using the Hidden Markov model and in (Von Krannichfeldt et al., 2021) using quantile regression, but they are limited to load demand and wind generation forecasting, respectively. In comparison, to (Álvarez et al., 2021) and (Von Krannichfeldt et al., 2021), we use our method to jointly estimate all the uncertain profiles as well as their uncertainty and subsequently, we employ the forecasts for the EMS application.

Summarising, this work presents two main contributions: (i) a probabilistic online learning method that estimates the mean and the variance of the uncertainty of all the predicted profiles: electricity price, load demand, renewable generation; (ii) a proactive scheduling strategy based on a stochastic MPC, where we require the amount of stored energy to fulfil the future predicted load demand with a probability greater than the one of fault occurrence, allowing us to avoid excessively conservative solutions.

Notation. We use subscripts to denote time instants, i.e. v_t is the vector v at time t. We denote $v_{k|t}$ the value of the variable v, k steps ahead of the time step t, i.e. at $t+k$. The estimation of the variable v is denoted as $\hat{v}$. So, the expected value of a variable v, available at time t, k steps ahead of time step t, i.e. at $t+k$, is denoted as $\hat{v}_{k|t}$. The variance of a variable v instead is denoted as $\sigma^2_{s,k|t} = \mathbb{E}\left[\left(s_{k|t} - \hat{s}_{k|t}\right)^2\right]$. We use bold variables to denote time sequences of N samples, namely $\mathbf{v}_{N|t} = \{v_{k|t}\}_{k\in\{0,\dots,N-1\}}$ is the sequence v from time step t to $t+N-1$.

2. ENERGY MANAGEMENT SYSTEM

2.1 System model

We consider four different agent types: loads, renewable generators, storage systems and connections to the utility grid. Renewable generators and loads are the power sources and sinks in the microgrid. The amount of power collectively produced by renewable generators at time t is denoted as P^r_t, whereas the power collectively drawn from the grid from loads at time t is denoted as P^l_t. Storage systems are modelled as first-order linear systems, as commonly done in the EMS literature (Parisio et al., 2014; Prodan et al., 2015):

$$s_{t+1} = (1-\nu)s_t + T_s P^s_t \tag{1}$$

where s_t is the state of charge at time t, $\nu \in [0,1]$ is the self-discharge rate, T_s is the controller sample time and the power P^s_t is the net power exchanged with the microgrid. The power P^s_t is the sum of the input $P^{s_{in}}_t$ and output $P^{s_{out}}_t$ power:

$$P^s_t = \eta_{in} P^{s_{in}}_t - \eta_{out} P^{s_{out}}_t \tag{2}$$

where $\eta_{in} \in [0,1], \eta_{out} \geq 1$ are the charging/discharging efficiencies, respectively. The limits on the storage power and charge are: $-P^s_M \leq P^s_t \leq P^s_M$, $s_m \leq s_t \leq s_M$, where P^s_M is the maximum power, s_M and s_m are the storage system's charge limits. The interconnection among the agents is modelled through the power balance constraint:

$$P^s_t + P^g_t = P^r_t - P^l_t \tag{3}$$

where P_t^g is the power exchanged with the utility grid ($P_t^g \geq 0$ when the microgrid is selling power). Thus, the microgrid can trade power with the utility grid, incurring a cost or earning at each time step computed as $\mathrm{C}_t = -p_t P_t^g$, where p_t is the electrical energy price. The goal of the EMS is to minimise the cumulative cost over all the time steps:

$$\mathrm{C} = \sum_{t=0}^{\infty} \mathrm{C}_t \tag{4}$$

while ensuring power delivery to loads in the case of a fault. This paper considers utility grid faults, however, extending the proposed method to other cases is straightforward. Other faults are investigated in (Casagrande et al., 2022; Prodan et al., 2015) where the problem of predicting the future profiles is not considered. In the case of a utility grid fault, the microgrid has to operate in island mode, hence resorting only to its storage capacity and local generation:

$$P_t^g = 0 \quad \forall\, t \in [\tau_i, \tau_f] \tag{5}$$

where τ_i and τ_f are the initial and final fault time.

2.2 Online Learning-based EMS

We now describe the controller, as designed in (Casagrande et al., 2023), which is extended for uncertainty estimation. The architecture is represented in Figure 1 and comprises two blocks: a predictor, on the left, online trained to forecast the future uncertain profiles, and an optimiser, on the right, that computes the power schedule. The input of

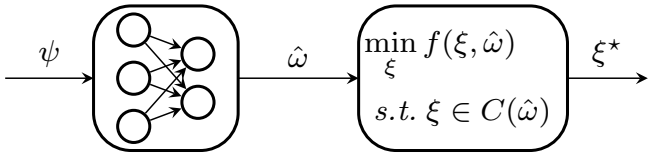

Fig. 1. The architecture of the EMS controller.

the block is a feature tensor ψ, the output is the prediction of the uncertain profiles $\hat{\omega}$. The optimiser block takes as input $\hat{\omega}$ and outputs the optimal value of the decision variable $\xi^\star$. The optimiser computes the optimal control actions ($\mathbf{P}^{s_{in}}_{T|t}$, $\mathbf{P}^{s_{out}}_{T|t}$). The predicted profiles are the future values of the electricity price, load demand and renewable generation over the prediction horizon: $\hat{\mathbf{p}}_{T|t}$, $\hat{\mathbf{P}}^l_{T|t}$, $\hat{\mathbf{P}}^r_{T|t}$. As ψ we use the past values of the profiles over the look-back window L: $\hat{\mathbf{p}}_{L|t-L}$, $\hat{\mathbf{P}}^l_{L|t-L}$, $\hat{\mathbf{P}}^r_{L|t-L}$.

The online training of the NN and the hyperparameters optimisation (HPO) are performed inspired by the method proposed in (Casagrande et al., 2023). In this paper, we enhance the method above to estimate the uncertainty of the forecasts as described in Section 3.1 and then use this estimate in a specifically designed stochastic MPC. At each time step, the NN performs two steps as in Figure 2. The training step, considering time sequences that are only in the past and computing the loss function $\mathcal{L}_t(\omega_t^{tr}, \hat{\omega}_t^{tr})$ using the predicted and the true profiles, which are available as all samples are in the past. The second is the test step, in which the NN predicts the future profiles and passes such information to the optimiser.

The optimisation problem solved at each time step t is the following:

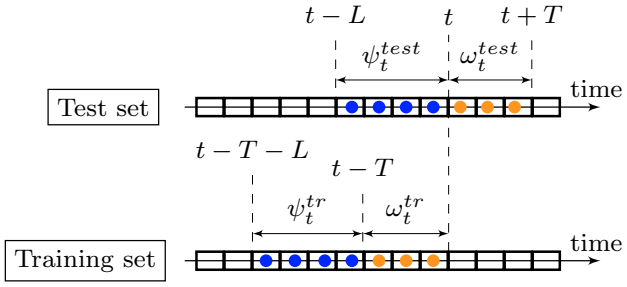

Fig. 2. Representation of the training and test sets. Blue and orange samples represent the NN's input and output respectively.

$$\min_{\mathbf{P}^{s_{in}}_{T|t}, \mathbf{P}^{s_{out}}_{T|t}} \quad \sum_{k=0}^{T-1} -\hat{p}_{k|t} P^g_{k|t} \tag{6a}$$

$$\text{s.t.} \quad s_{k+1|t} = (1-\nu) s_{k|t} + T_s P^s_{k|t} \tag{6b}$$

$$P^s_{k|t} = \eta_{in} P^{s_{in}}_{k|t} - \eta_{out} P^{s_{out}}_{k|t} \tag{6c}$$

$$-P^s_M \leq P^s_{k|t} \leq P^s_M \tag{6d}$$

$$s_m \leq s_{k|t} \leq s_M \tag{6e}$$

$$P^g_{k|t} + P^s_{k|t} = \hat{P}^r_{k|t} - \hat{P}^l_{k|t} \tag{6f}$$

$$s_{0|t} = s_t \tag{6g}$$

$$s_{k+1|t} \geq \tilde{s}^\tau_{k+1|t} \tag{6h}$$

The objective function (6a) is the finite horizon approximation of (4) using the predicted price. The dynamics of the storage system appear in (6b) and (6c). Constraints (6d) and (6e) are the storage limits and (6f) is the power balance. The state feedback is (6g). Constraints (6h) implement the proactive scheduling strategy. The constraint enforces the storage charge to be greater than a pre-defined charge, enough to supply loads in case of faults for τ steps. Depending on the storage capacity and the load need, the amount of backup energy $\tilde{s}^\tau_{k|t}$ can be computed differently. For example, some methods in the literature require the backup energy to be greater than the total energy demand of the loads for the following τ steps without taking into account the renewable power production. The renewable power production can be taken into account as:

$$\tilde{s}^\tau_{k|t} = \sum_{i=0}^{\tau} T_s [\hat{P}^r_{k+i|t} - \hat{P}^l_{k+i|t}] \tag{7}$$

assuming the load is deferrable. In the following, we will assume that the storage has enough capacity and power limits to enforce the backup energy constraint. It should be noted that Eq. (7) uses the forecasts of renewable and load power profiles since they are not known in advance. One of the goals of this work is enforcing (6h) with a certain level of robustness given the prediction uncertainty. An outage management strategy, like the one presented in (Casagrande et al., 2022; Haessig et al., 2019), can be integrated with the proposed method by modifying the optimisation problem when a fault occurs. Once the optimal solution of Problem (6a)-(6h) is computed, the control law is defined as $P^{s_{in}}_t = P^{s_{in}\star}_{0|t}$, $P^{s_{out}}_t = P^{s_{out}\star}_{0|t}$. The state of the storage evolves to s_{t+1} as presented in Section 2.1 according to Eqs. (1) and (2), as well as the power exchanged with the utility grid P^g_t, following

Eq. (3). The microgrid incurs a cost at each time step which determines the overall cost computed as Eq. (4).

3. RESILIENT STOCHASTIC EMS

The previously presented method assumes a fault can happen at each time step but it does not consider the probability of fault occurrence. It also does not consider uncertainty in the future load demand and renewable generation. Therefore, when the fault probability is low, we can tolerate violating such constraint due to uncertainty since it is very likely that the backup energy will not be used. Hence, we reformulate constraint (6h) as:

$$pr\big(s_{k+1|t} \leq \tilde{s}^{\tau}_{k+1|t}\big) \leq \pi_t \tag{8}$$

where $\pi_t \in [0;1]$ represents an acceptable probability level of constraint violation, dependent on time. By setting π_t as the complementary probability of fault occurrence, the EMS will store the minimum amount of required backup energy with high probability. Hence it is necessary to reformulate (8) in a deterministic way. Namely constraint (6h) has to be tightened by reformulating (8) as $s_{k+1|t} \geq \tilde{s}^{\tau}_{k+1|t} + \delta^{\pi}_{k+1|t}$, where $\delta^{\pi}_{k+1|t}$ is the tightening value. In the following, we first extend the online learning algorithm to estimate uncertainties, then we compute $\delta^{\pi}_{k+1|t}$ by reformulating (8).

3.1 Uncertainty estimation

The online learning method is extended to estimate the predictions' expected value and variance over the prediction horizon.

Assumption 1. It is assumed the future uncertain profiles are Gaussian variables, as in (Álvarez et al., 2021). In particular, for load and renewable generation $P^l_{k|t} \sim \mathcal{N}(\hat{P}^l_{k|t}, \hat{\sigma}^2_{l,k|t})$, $P^r_{k|t} \sim \mathcal{N}(\hat{P}^r_{k|t}, \hat{\sigma}^2_{r,k|t})$, where $\hat{P}^*_{k|t}$, $\hat{\sigma}^2_{*,k|t}$ denote the expected value and variance respectively.

Instead of estimating $3\times T$ variables, i.e. only the expected value, the NN estimates $2\times 3\times T$ variables, i.e. the expected value and the variance. In general terms, we denote the predicted mean and variance of the uncertain profiles as $\hat{\omega}_{k|t}$ and $\hat{\sigma}^2_{k|t}$, respectively. Therefore, the likelihood of the predicted profiles is $pr\big(\omega_{k|t}|\hat{\omega}_{k|t}, \hat{\sigma}_{*,k|t}\big) = \mathcal{N}(\hat{\omega}_{k|t}, \hat{\sigma}_{*,k|t})$, where $\hat{\omega}_{k|t}$ is the actual value of the uncertain profile at time $k+t$. The NN learns the parameters of the Gaussian distribution by minimising the negative log-likelihood of the predicted profiles as:

$$\mathcal{L}_t(\omega_t, \hat{\omega}_t, \hat{\sigma}_t) = -\log\Big(pr\big(\omega_{k|t}|\hat{\omega}_{k|t}, \hat{\sigma}_{*,k|t}\big)\Big) = \frac{1}{2}\log(2\pi\hat{\sigma}_{*,k|t}) + \frac{(\omega_{k|t} - \hat{\omega}_{k|t})^2}{2\hat{\sigma}^2_{*,k|t}} + C \tag{9}$$

C is a constant term independent of the output. Hence, the NN empirically learns to predict the expected value and the variance of uncertain profiles.

3.2 Chance constraint reformulation

We now use the estimated prediction uncertainty to reformulate the chance constraint (8) as in (Farina et al., 2013) using Cantelli's inequality:

$$pr\big(x - \hat{x} \leq \lambda\big) \leq \frac{\hat{\sigma}^2_x}{\hat{\sigma}^2_x + \lambda^2} \tag{10}$$

where $\hat{x}$ and $\hat{\sigma}^2_x$ are the expected value and variance of x, $\lambda \in \mathbb{R}$. First, the state variance must be computed to use (10) for reformulating (8).

Assumption 2. It is assumed that the state, renewable generation and load profiles are uncorrelated, i.e. $\mathbb{E}[(s_k - \hat{s}_k)(P^l_k - \hat{P}^l_k)] = 0$, $\mathbb{E}[(s_k - \hat{s}_k)(P^r_k - \hat{P}^r_k)] = 0$, $\mathbb{E}[(P^r_k - \hat{P}^r_k)(P^l_k - \hat{P}^l_k)] = 0$.

We propagate the state variance over the prediction horizon, i.e. the dynamics of the state variance. By combining the storage dynamics (1), the power balance (3) and the fault model (5) we obtain:

$$\begin{aligned} s_{k+1} - \hat{s}_{k+1} = \\ (1-\nu)s_{k|t} + T_s P^s_{k|t} - (1-\nu)\hat{s}_{k|t} - T_s\hat{P}^s_{k|t} = \\ (1-\nu)(s_{k|t} - \hat{s}_{k|t}) + T_s(P^r_{k|t} - \hat{P}^r_{k|t}) + T_s(P^l_{k|t} - \hat{P}^l_{k|t}) \end{aligned}$$

The state variance is $\sigma^2_{s,k+1|t} = \mathbb{E}[(s_{k+1} - \hat{s}_{k+1})^2]$, hence by considering Assumption 2, we obtain:

$$\sigma^2_{s,k+1|t} = (1-\nu)^2\sigma^2_{a,k|t} + T_s^2(\hat{\sigma}^2_{r,k|t} + \hat{\sigma}^2_{l,k|t}) \tag{11}$$

which is the dynamics of the state variance. The constraint (8) is reformulated as a deterministic constraint employing (10) and the procedure explained in (Farina et al., 2013):

$$\hat{s}_{k+1|t} \geq \tilde{s}_{k+1|t} + \sigma^2_{s,k+1|t}\sqrt{\frac{1-\pi}{\pi}} \tag{12}$$

The first term is the predicted backup energy for fault resilience and the second term considers the predicted variance of the state. The resulting optimisation problem is:

$$\min_{\mathbf{P}^{s_{in}}_{T|t}, \mathbf{P}^{s_{out}}_{T|t}} \quad \sum_{k=0}^{T-1} -\hat{p}_{k|t}P^g_{k|t} \tag{13a}$$

$$\text{s.t.} \quad \hat{s}_{k+1|t} = (1-\nu)\hat{s}_{k|t} + T_s P^s_{k|t} \tag{13b}$$

$$\sigma^2_{s,k+1|t} = (1-\nu)^2\sigma^2_{s,k|t} + T_s^2(\sigma^2_{r,k|t} + \sigma^2_{l,k|t}) \tag{13c}$$

$$P^s_{k|t} = \eta_{in}P^{s_{in}}_{k|t} - \eta_{out}P^{s_{out}}_{k|t} \tag{13d}$$

$$-P^s_M \leq P^s_{k|t} \leq P^s_M \tag{13e}$$

$$s_m \leq s_{k|t} \leq s_M \tag{13f}$$

$$P^g_{k|t} + P^s_{k|t} = \hat{P}^r_{k|t} - \hat{P}^l_{k|t} \tag{13g}$$

$$s_{0|t} = s_t, \quad \sigma^{2,s}_{0|t} = 0 \tag{13h}$$

$$\hat{s}_{k+1|t} \geq \tilde{s}_{k+1|t} + \sigma^2_{s,k+1|t}\sqrt{\frac{1-\pi}{\pi}} \tag{13i}$$

where the initial condition (13h) for the state variance is set to zero as the current state s_t is known.

4. EXPERIMENTAL RESULTS

The datasets employed in the following experiments are taken from the *EMSx* benchmark dataset (Le Franc et al., 2021) for the power profiles and the *ENTSO-E Transparency Platform* dataset (Hirth et al., 2018) for the price. The power profiles comprise a PV plant as a renewable generator and an industrial site as a load. As NN we employed a network composed of a single LSTM layer

with 48 hidden units followed by a dense layer. The NN has been pre-trained on industrial site 10 and the hyperparameters have been set using the HPO procedure described in (Casagrande et al., 2023) on the pre-training dataset. Pre-training is suggested to warm-start the online learning algorithm and transfer the knowledge from one site to another. The controller is then tested on industrial site 12. The system has been simulated for 15400 steps with a sampling time $T_s = 1$h (1.8 years). Other simulation parameters are: $T = 24$, $L = 168$, $\nu = 0.0042$, $\eta_{in} = 0.95$, $\eta_{out} = 1.05$, $s_m = 80$kWh, $s_M = 800$kWh, $P^s_M = 500$kW, $\tau = 1$h. The employed code is available on GitHub at `https://github.com/vittpi/ol-ems`.

4.1 Uncertainty estimation

Figure 3 shows the results on the three unknown profiles. The blue lines are the ground truth, P^l_t, P^r_t, p_t, the orange lines are the expected value of the first predicted sample, $\hat{P}^l_{0|t}$, $\hat{P}^r_{0|t}$, $\hat{p}_{0|t}$, and the orange area represents the 1-standard deviation band $\hat{P}^l_{0|t} \pm \hat{\sigma}_{l,0|t}$, $\hat{P}^r_{0|t} \pm \hat{\sigma}_{r,0|t}$, $\hat{p}_{0|t} \pm \hat{\sigma}_{p,0|t}$. The ground truth value is within the uncertainty band for most of the represented samples. However, sometimes, it has some unexpected behaviours, e.g. the load profiles have a sudden spike on the 1st of September. The uncertainty band of the electricity price is broader than the other two, suggesting that it is more difficult to predict. The results of the uncertainty estimation are numerically assessed in Table 1 where the percentage of samples that lie within one, two and three standard deviations over all the simulation steps are computed. The obtained values are in line with the 68-95-99.7 rule.

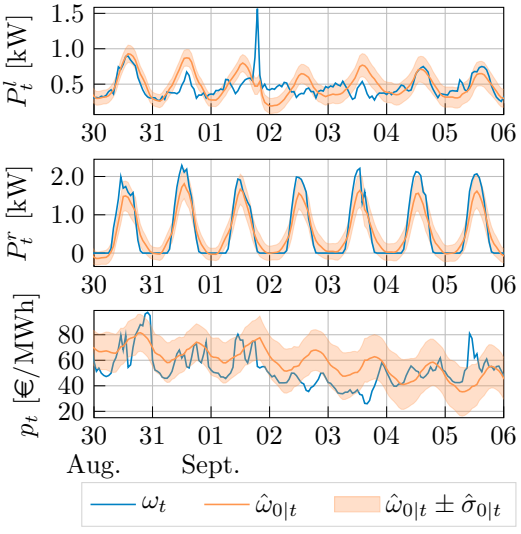

Fig. 3. Ground truth, expected value and uncertainty band of the unknown profiles.

4.2 Resilient EMS

Three effects of the implementation of the proactive scheduling strategy are shown: (i) the amount of backup energy is affected by the uncertainty estimation results, i.e. more energy is stored in moments of higher uncertainty; (ii) the amount of backup energy depends on the fault probability, i.e. when the fault probability is higher, more energy is stored; (iii) there is a trade-off between resilience and economic performance. The first effect is clear from Fig. 4 that shows the constraint tightening limit, for $k = 0$, over some simulation steps. By comparing Fig. 4 with Fig. 3, we see that the constraint tightening is greater in moments of higher uncertainty. The constraint has a periodic behaviour with a peak at midday due to the uncertainty band of renewable energy production, which is zero during the night but may have different values during the day. The second effect is also evident from Fig. 4, showing the constraint tightening for different fault probability levels π_t in simulations where we assume the fault probability is constant over time. More energy is stored when the fault probability π_t is higher. In the first row of Table 2, the percentage of times in which the stored energy is lower than the required backup energy is given, and this value decreases as π_t increases, as the controller becomes more robust to potential fault occurrence. Thirdly, the trade-off between resilience and economic performance is evident from the second row of Table 2. As the amount of backup energy and less storage capacity can be used for the normal EMS operation, the total cost computed over all the simulation steps increases. However, in this scenario, we kept π_t constant for all simulation steps. This value, however, can be changed over time as the probability of fault occurrence changes, as shown in the results in Fig. 5. The second effect, i.e. the amount of backup energy depends on the fault probability, is also evident from Fig. 5 that shows the experimental results in a simulation scenario where π_t changes over time. The top plot represents the storage state s_t and the true value of the backup energy computed as in Eq. (7) with the true values of load demand and renewable generation. The middle plot represents the constraint tightening, and the bottom plot represents the fault probability. As the fault probability increases over time, the constraint tightening increases too while fluctuating in response to the predictions and uncertainty estimation. Moreover, as the fault probability increases, from the top plot, we can see that the low values that the state periodically reaches have an increasing trend due to the constraint tightening.

Table 1. Percentage of samples, for each unknown profile, that lie within 1, 2 and 3 σ and comparison with the theoretical result.

Interval	Price	Load	PV	Average	68-95-99.7 rule
σ	70.4%	65.3%	73.0%	69.6%	68.3%
2σ	93.4%	92.7%	94.3%	93.5%	95.5%
3σ	98.3%	98.3%	99.4%	98.5%	99.7%

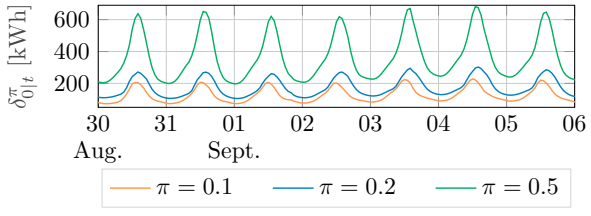

Fig. 4. Backup energy constraint tightening limits evolution for different constant probability levels over time.

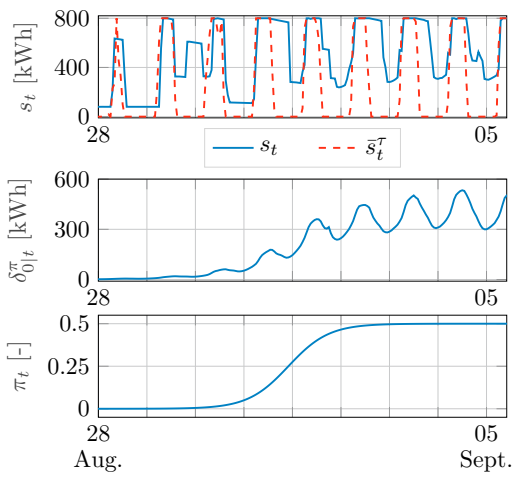

Fig. 5. Simulation results obtained when the fault probability starts to increase.

Table 2. Results on violating the chance constraint and total cost for different probability levels.

π_t	0.1	0.2	0.5
$s_t \leq \tilde{s}_t^\tau$ [%]	15.85 ± 1.26	13.77 ± 0.19	10.25 ± 0.10
C [€]	$67,126 \pm 109$	67.450 ± 159	$67,773 \pm 366$

5. CONCLUSION

This paper proposes a novel proactive scheduling strategy for microgrid energy management to ensure fault resilience during a utility grid outage. The proposed EMS consists of an online learning-based predictor and a stochastic MPC. The predictor is trained online to forecast the mean and the variance of the future profiles. The optimiser uses this information to compute the power schedule to optimise economic performance. Proactive scheduling is enforced as a chance constraint of the optimisation problem to consider the prediction uncertainty and probability of fault occurrence. Simulation results show that a reliable estimation of the prediction uncertainty can be obtained, and the proactive scheduling constraint enhances resilience against faults. As for future work, we will extend the method to consider chance constraints not only in the system state but also in the system input.

REFERENCES

Álvarez, V., Mazuelas, S., and Lozano, J.A. (2021). Probabilistic load forecasting based on adaptive online learning. *IEEE Transactions on Power Systems*, 36(4), 3668–3680.

Bernardi, E., Morato, M.M., Mendes, P.R., Normey-Rico, J.E., and Adam, E.J. (2021). Fault-tolerant energy management for an industrial microgrid: A compact optimization method. *International Journal of Electrical Power & Energy Systems*, 124, 106342.

Casagrande, V. and Boem, F. (2022). A distributed scenario-based stochastic MPC for fault-tolerant microgrid energy management. *IFAC-PapersOnLine*, 55(6), 704–709.

Casagrande, V., Ferianc, M., Rodrigues, M., and Boem, F. (2023). An online learning method for microgrid energy management control. In *2023 31st Mediterranean Conference on Control and Automation (MED)*, 263–268. IEEE.

Casagrande, V., Prodan, I., Spurgeon, S.K., and Boem, F. (2022). Resilient microgrid energy management algorithm based on distributed optimization. *IEEE Systems Journal*.

Farina, M., Giulioni, L., Magni, L., and Scattolini, R. (2013). A probabilistic approach to model predictive control. In *52nd IEEE conference on decision and control*, 7734–7739. IEEE.

Haessig, P., Bourdais, R., Guéguen, H., et al. (2019). Resilience in energy management system: A study case. *IFAC-PapersOnLine*, 52(4), 395–400.

Hirth, L., Mühlenpfordt, J., and Bulkeley, M. (2018). The entso-e transparency platform–a review of europe's most ambitious electricity data platform. *Applied energy*, 225, 1054–1067.

Hussain, A., Bui, V.H., and Kim, H.M. (2019). Microgrids as a resilience resource and strategies used by microgrids for enhancing resilience. *Applied energy*, 240, 56–72.

Jongerden, M.R., Hüls, J., Remke, A., and Haverkort, B.R. (2016). Does your domestic photovoltaic energy system survive grid outages? *Energies*, 9(9), 736.

Khodaei, A. (2014). Resiliency-oriented microgrid optimal scheduling. *IEEE Transactions on Smart Grid*, 5(4), 1584–1591.

Lasseter, R. (2002). Microgrids. *2002 IEEE Power Engineering Society Winter Meeting. Conference Proceedings (Cat. No.02CH37309)*, 1, 305–308. doi:10.1109/PESW.2002.985003. URL `http://ieeexplore.ieee.org/document/985003/`.

Le Franc, A., Carpentier, P., Chancelier, J.P., and De Lara, M. (2021). EMSx: a numerical benchmark for energy management systems. *Energy Systems*, 1–27.

Panteli, M. and Mancarella, P. (2015). Influence of extreme weather and climate change on the resilience of power systems: Impacts and possible mitigation strategies. *Electric Power Systems Research*, 127, 259–270.

Panteli, M., Trakas, D.N., Mancarella, P., and Hatziargyriou, N.D. (2016). Boosting the power grid resilience to extreme weather events using defensive islanding. *IEEE Transactions on Smart Grid*, 7(6), 2913–2922.

Parisio, A., Rikos, E., and Glielmo, L. (2014). A model predictive control approach to microgrid operation optimization. *IEEE Transactions on Control Systems Technology*, 22(5), 1813–1827.

Pashajavid, E., Shahnia, F., and Ghosh, A. (2015). Development of a self-healing strategy to enhance the overloading resilience of islanded microgrids. *IEEE transactions on smart grid*, 8(2), 868–880.

Prodan, I., Zio, E., and Stoican, F. (2015). Fault tolerant predictive control design for reliable microgrid energy management under uncertainties. *Energy*, 91, 20–34.

Tobajas, J., Garcia-Torres, F., Roncero-Sánchez, P., Vázquez, J., Bellatreche, L., and Nieto, E. (2022). Resilience-oriented schedule of microgrids with hybrid energy storage system using model predictive control. *Applied Energy*, 306, 118092.

Von Krannichfeldt, L., Wang, Y., Zufferey, T., and Hug, G. (2021). Online ensemble approach for probabilistic wind power forecasting. *IEEE Transactions on Sustainable Energy*, 13(2), 1221–1233.